Experimental Investigation of Solid Rocket Motors for a Student Sounding Rocket

Yannick Lecomte^{1,2†}, Riccardo Gelain^{1,3†}, Mariano Di Matteo^{1,3} and Patrick Hendrick¹

¹Université libre de Bruxelles

50 Avenue F.D. Roosevelt, 1050 Brussels, Belgium

²von Karman Institute for Fluid Dynamics

72 Waterloosesteenweg, 1640 Sint-Genesius-Rode, Belgium

³ Royal Military Academy

30 Avenue de la Renaissance, 1000 Brussels, Belgium

yannick.lecomte@vki.ac.be · riccardo.gelain@mil.be · mariano.di.matteo@ulb.be · patrick.hendrick@ulb.be

†Corresponding authors

Abstract

The Aero-Thermo-Mechanics (ATM) department of Université Libre de Bruxelles (ULB) has been actively conducting research in the field of space propulsion for several years, with a particular focus on experimental investigation on hybrid propulsion. In September 2023, a group of Belgian university students has formed a student team called Be-Rocket, with the goal of working on amateur rocketry and developing their own sounding rockets and propulsion systems. The team groups students coming from different specializations in different Belgian universities. The initiative lead to the development of the first rocket of the team, the Bossart One, powered by a commercially available Solid Rocket Motor (SRM), designed to reach an altitude of 3 km and to adhere to the regulations of the EuRoC (European Rocketry Challenge). The rocket has been qualified in November 2024, with a first successful launch from the Elsenborn military site.

This paper focuses on the selection of a SRM based on the rocket specification criteria, in particular for the lower apogee of 1 km selected for the first qualification launch, and the subsequent experimental investigation of its performances, through the creation of a new SRM test bench for the ATM department.

First, a simplified apogee prediction model has been developed to narrow down the wide range of motor models, and the results have been compared with the software *OpenRocket*. The paper then discussed the design and manufacturing of a dedicated and adaptable test bench for static firing testing of SRMs, along with acquisition systems for thrust and temperature measurements. This overall setup has been validated by comparing the experimental thrust data collected with the manufacturer-provided data. Moreover, some failed tests highlighted the importance of defining and following strict safety protocols, providing precious lessons for the team.

1. Introduction

In September 2023, a group of Belgian university students founded the inter-university team *Be-Rocket*, with the aim of designing and building amateur sounding rockets from scratch, while developing hands-on experience in aerospace engineering [1]. The team brings together students from four institutions, ULB, VUB, KU Leuven, and ULiège, and benefits from the technical support of the Royal Military Academy (RMA), particularly in ballistics and access to military testing facilities. The team's primary goal is to participate in the European Rocketry Challenge (EuRoC) [3], joining student rocketry teams from across Europe in a competition. The team aims to compete in the category targeting an apogee altitude of 3 km. However, for its inaugural year, the team has set a first objective: a proof-of-concept launch targeting an apogee of 1 km. The team's efforts are therefore focused on the design, construction, and launch of a first prototype rocket, *Bossart-I*, serving as a stepping stone toward full participation in EuRoC.

The propulsion system selected for *Bossart-I* is a solid rocket motor (SRM). While hybrid and liquid propulsion systems are common in modern aerospace applications and widely adopted by student teams [8, 4, 2], SRMs remain in use in several contemporary launch vehicles, such as ESA's Ariane 6, which employs solid boosters during lift-off. Their simplicity, requiring no fluid circuits or pressurization systems, makes them robust, reliable, and well-suited

for experimental handling [5]. Moreover, the availability of certified commercial SRMs simplifies integration into a student-led project.

The work presented in this paper is structured into several key steps, as summarized in Figure 1, with the overarching objective of launching a student-built sounding rocket. The first step involves the selection of a suitable solid rocket motor through an iterative process, supported by a simplified apogee prediction model. This selection is guided by the team's main objective to launch a rocket at 3 km apogee objective. However, the selected model for this work align with the inaugural launch targeting 1 km. Once the motor is selected, it must be tested for both validation and operational readiness using a dedicated test bench, which was designed and constructed by the Aero-Thermo-Mechanics (ATM) department of Université Libre de Bruxelles (ULB). Finally, the results of the static firing tests are discussed in detail in the Results section.

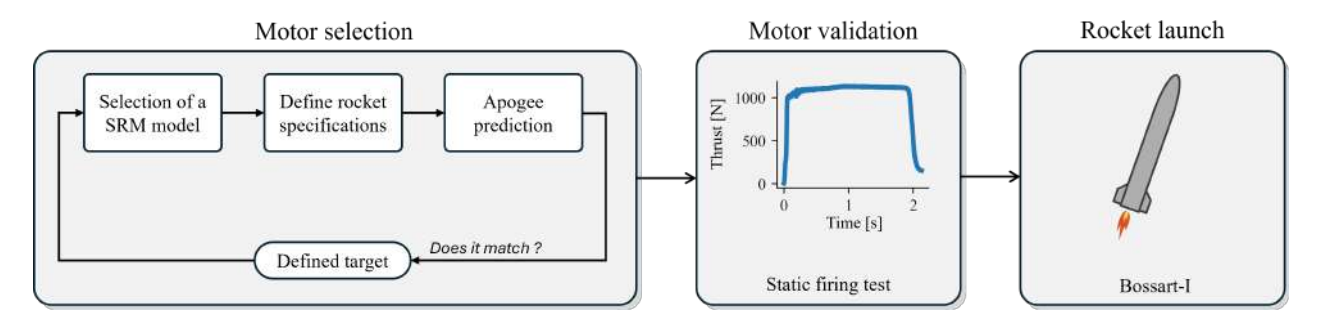


Figure 1: Full process steps for the propulsion system of Bossart-I.

2. Methodology

2.1 Motor selection

Solid rocket motors (SRMs) combine fuel and oxidizer into a single solid structure known as the propellant grain. Thrust is generated by the combustion of the grain, which initiates from its internal cavity, typically hollow and cylindrical [5]. More advanced configurations use alternative cavity shapes such as star, C-star, finocyl, or wagon wheel geometries to modulate the burning surface area over time and shape the thrust profile. The combustion performance also depends on the chemical composition of the propellant [10]. Overall, the four main parameters that determine the thrust-time profile of a given SRM configuration are: the grain's length, its external diameter, the geometry of the internal cavity (grain shape), and the propellant formulation [7].

The design of the rocket follows an iterative process, where propulsion, structure, payload, recovery, and aerodynamic parameters are closely interdependent. The previous factors significantly influence the overall configuration of the rocket. For example, a longer motor may provide a higher total impulse and longer burn time, potentially increasing the apogee, but it also leads to a longer and heavier rocket with increased drag. Since the apogee is the primary performance target it is essential to quantify how different motor configurations impact it. This is illustrated in Figure 1, where the apogee target represents the validation key of the iterative process.

Among the available commercial options, the off-the-shelf motor selected for this project is manufactured by $Cesaroni\ Technology\ Inc$. This choice was based on the availability of their products through European resellers and their compliance with EuRoC competition requirements. The $Pro-X^{\textcircled{@}}$ line from $Cesaroni\ Technology\ Inc$. offers a wide range of SRMs with varying dimensions, grain configurations, and thrust profiles, with diameters ranging from 24 mm to 150 mm. Open-source software such as OpenRocket can provide apogee predictions with a certain degree of design parameter refinement. However, implementing a complete rocket design in the software for every motor configuration can be time-consuming. To support the selection process across the wide range of available models, a simplified apogee prediction tool was developed that automatically adapts the rocket design to each motor's parameters, enabling rapid evaluation of the entire catalogue.

2.1.1 Altitude Prediction Model

The flight of a rocket can be divided into distinct phases from lift-off to landing, as illustrated in Figure 2. For altitude prediction, only the boost and coast phases are relevant, as they represent, respectively, the thrust-driven and free-flight motion. The following model is derived from the investigation of Lee *et al.* [6].

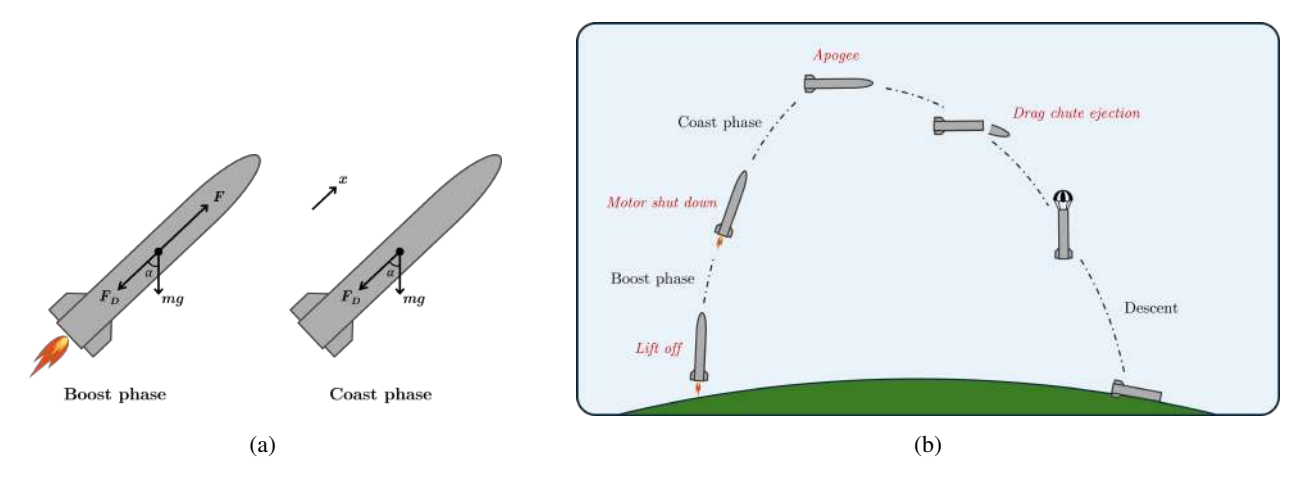


Figure 2: (a) Force balance on the rocket during the boost and coast phase, and (b) flight phases.

Boost Phase

During the boost phase, the rocket is subjected to thrust, gravity, and aerodynamic drag. Newton's second law gives:

$$F - F_D - mg = m\frac{dv}{dt},\tag{1}$$

where F is the thrust force generated by the propulsion system, F_D is the aerodynamic drag force, m is the instantaneous mass of the rocket, g is the gravitational acceleration, and v is the rocket's velocity. The drag force is modeled as $F_D = \frac{1}{2}\rho v^2 C_D A$, where ρ is the air density, C_D is the drag coefficient, and A is the reference cross-sectional area of the rocket. For convenience, this expression is rewritten as $F_D = kv^2$, where $k = \frac{1}{2}\rho C_D A$ encapsulates the aerodynamic parameters.

To facilitate an analytical solution, all time-dependent quantities during the boost phase are replaced with their average values. The average thrust is denoted by \bar{F} , the average rocket mass during the burn by m_{bo} , and the air density included in k is also treated as constant. Equation (1) becomes:

$$dt = \frac{m_{bo}}{k(q_{bo}^2 - v^2)} dv$$
, with $q_{bo}^2 = \frac{\bar{F} - m_{bo}g_x}{k}$. (2)

Integrating from t = 0 to t_b yields the burn time relation expressed in equation (3):

$$t_b = \frac{m_{bo}}{2q_{bo}k} \ln\left(\frac{q_{bo} + v_{bo}}{q_{bo} - v_{bo}}\right),\tag{3}$$

or equivalently, defining $p = \frac{2kq_{bo}}{m_{bo}}$, the velocity at the end of the boost is given in equation (4):

$$v_{bo} = q_{bo} \frac{1 - e^{-pt_b}}{1 + e^{-pt_b}}. (4)$$

To find the altitude gained during the boost, the relation (5) is used

$$dh = \frac{m_{bo}v}{k(q_{bo}^2 - v^2)}dv, (5)$$

which integrates to:

$$h_{bo} = \frac{m_{bo}}{2k} \ln \left(\frac{q_{bo}^2}{q_{bo}^2 - v_{bo}^2} \right). \tag{6}$$

Coast Phase

Once the thrust ceases, the rocket continues to climb under the influence of gravity and drag:

$$-kv^2 - mg_x = mv\frac{dv}{dh}. (7)$$

Defining $q_{co}^2 = \frac{m_{co}g_x}{k}$, where m_{co} is the post-burn mass, the relation (8) is obtained:

$$dh = \frac{m_{co}v}{k(-q_{co}^2 - v^2)}dv. (8)$$

Integration from $v = v_{bo}$ to v = 0 gives the coast altitude expressed by equation (9):

$$h_{co} = \frac{m_{co}}{2k} \ln \left(\frac{q_{co}^2 + v_{bo}^2}{q_{co}^2} \right). \tag{9}$$

The total altitude reached by the rocket is the sum of both phases:

$$h_{tot} = h_{bo} + h_{co}. (10)$$

2.1.2 Final selection

First, the implementation of the apogee prediction model across the full Pro-X[®] catalogue led to the selection of the PRO75 line, corresponding to motors with a diameter of 75 mm. Based on this choice, and in collaboration with all sections of Be-Rocket, a first iteration of the complete rocket specifications was established.

Once the motor selection was narrowed to the PRO75 line, the simplified apogee prediction model was directly compared with *OpenRocket* simulations, as the reduced number of configurations made verification more manageable. Figure 3 shows the results of both models across various PRO75 motors. Based on this analysis, the PRO75 5880 - 5G motor was selected for the 3 km target. To define a suitable configuration for the reduced 1 km mission, the total length and mass of the 3 km rocket, detailed in Table 1, were kept constant, and the simplified model was evaluated over motors smaller than the PRO75 5880. In the final configuration, the motor was shortened to lower the apogee to approximately 1 km, while preserving the full rocket architecture. The unused internal volume was filled with a machined aluminum insert to match the mass of the removed grains, maintaining the rocket's mass distribution and dynamic behavior and allowing future upgrades without redesigning the airframe.

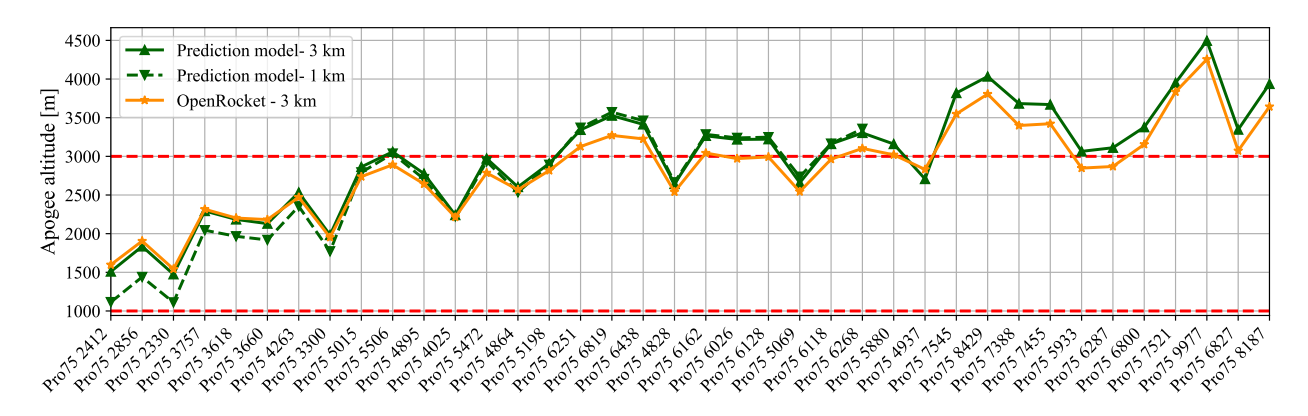


Figure 3: Comparison of the altitude prediction between the simplified apogee prediction model and *OpenRocket*.

The results for the 1 km target prediction are shown as a dashed line in Figure 3, illustrating a clear trend of decreasing apogee with smaller motor sizes. The motor selected for this objective is the PRO75 2412 - 2G, as its predicted apogee closely aligns with the 1 km requirement. Additionally, to validate the performance of the test bench and the data acquisition procedure, a smaller and more cost-effective SRM, the PRO38 5401 - 4G, with a diameter of 38 mm, was included in the experimental campaign. The final motor selection is summarized in Table 2, listing the two motors to be acquired and an additional one reserved for the future 3 km launch objective.

Specification type	Parameters	Value
Lengths	$L_{ m propulsion\ bay}$	757 mm
	$L_{ m avionics\ bay}$	300 mm
	$L_{ m recovery\ bay}$	500 mm
	$L_{ m payload\ bay}$	114 mm
	$L_{ m fairing\ bay}$	294 mm
Weights	$m_{ m payload}$	2 kg
	$m_{ m telemetry}$	0.025 kg
	$m_{ m avionics}$	0.075 kg
	$m_{ m battery}$	0.2 kg
	$m_{ m bulkheads}$	$0.460 \mathrm{kg}$
	$m_{ m structure}$	3.78 kg
	$m_{ m skin}$	0.257 kg
	$m_{ m motor}$	5.698 kg

Table 1: Rocket specifications at design stage for the 3 km target.

Table 2: Final motor selection.

Skin thickness

Launch angle, α

Drag coefficient, C_d

3 mm

0.3395 [-]

 85°

Model	Simulated apogee	
PRO38 5401 - 4G	-	Assessment of the test bench
PRO75 2412 - 2G	1114 m	Proof-of-concept launch with Bossart-I
PRO75 5880 - 5G	3159 m	Future preparative launch for EuRoC

2.2 Testing facility

Other

The selected SRM must be tested and validated before its integration into the final rocket. This step provides essential hands-on experience with the motor's installation, assembly, and operation. Despite manufacturer provided thrust curves, static tests remain critical to validate performance and assess ignition reliability. To support this, a dedicated test facility has been set up at in the ULB rocket propulsion testing facility, hosted at Beauvechain Air Base.

The static test bench was specifically designed and built for this project, based on a set of constraints and requirements. Due to the configuration of the site, horizontal testing was necessary, requiring the bench to be mounted on a table and aligned with a horizontal exhaust duct. To support future research by Be-Rocket and the ATM department of ULB, the bench is designed to accommodate a wide range of SRMs sizes, including the different specifications of the *Cesaroni*'s catalogue.

As a result, Figure 4 presents the final test bench. A sliding plate is mounted on two longitudinal rails, allowing movement along the thrust axis. The plate includes multiple mounting holes to accommodate motors of various sizes, which are secured using custom-made clamping pieces. During firing, the plate transfers thrust to a load cell with a maximum loading of 10 kN, while the reaction force is absorbed by oblique support bars.

The test facility is equipped with National Instruments (NI) hardware. The thrust signal is amplified, digitized via a DAQ card, and recorded by the main computer. The ignition signal is simultaneously sent to the igniter. Data is acquired at a sampling rate of 1500 Hz. A custom LabVIEW interface was developed, incorporating a safety checklist that prevents ignition unless all checkpoints are manually verified.

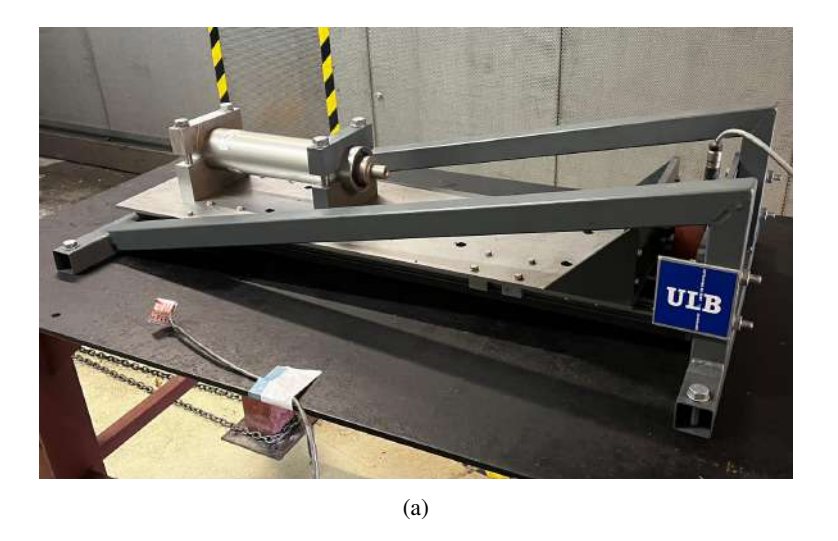




Figure 4: Static test bench installed at the test facility: (a) overall setup, (b) close-up of the 10 kN load cell.

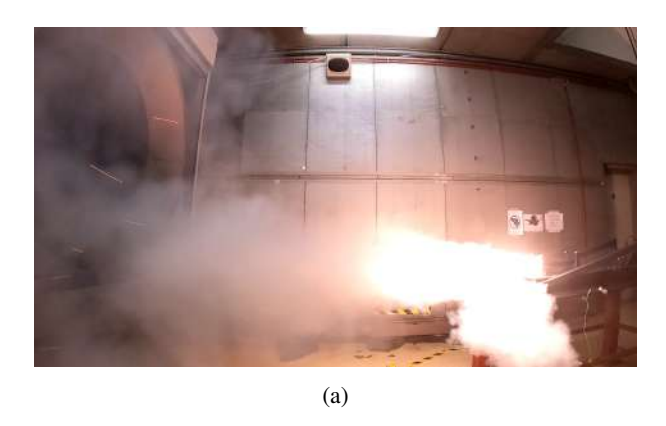
3. Results & Discussions

This section presents the results of static firing tests conducted on the PRO38 and PRO75 solid rocket motors (SRMs). The objective is to validate motor performance, assess data acquisition reliability, and compare the measured thrust curves with the manufacturer's specifications.

Prior to testing, it was essential to establish a detailed test procedure due to the significant safety risks associated with the handling of SRMs. *Cesaroni* motors contain energetic materials such as ammonium perchlorate and black powder, which are classified under the Globally Harmonized System of Classification and Labelling of Chemicals (GHS) as H204: "Fire or projection hazard". The Safety Data Sheet (SDS) provided by *Cesaroni* outlines all necessary precautionary measures. Accordingly, a dedicated test protocol was developed for this campaign to ensure safety operations.

The full set of purchased motors was tested over the course of two test campaigns conducted at the facility. The initial tests were performed on the smaller model, the PRO38, with the objective of validating the mechanical integrity of the test bench and verifying the functionality of the data acquisition system. These initial trials were successful, confirming the operational readiness of the test setup. However, two tests (Test 4 and Test 5) were invalidated due to handling errors during setup, and their data were discarded. As a result, the test matrix for the PRO38 includes two missing entries, that will be discussed in the following analysis.

Subsequently, the larger PRO75 motor were tested successfully without incident. Figure 5 shows images captured during the firing of both SRMs model. The right-hand image clearly illustrates the longer and more intense exhaust plume of the PRO75 motor, while both motors display a similar conical flame shape characteristic of their nozzle geometries.



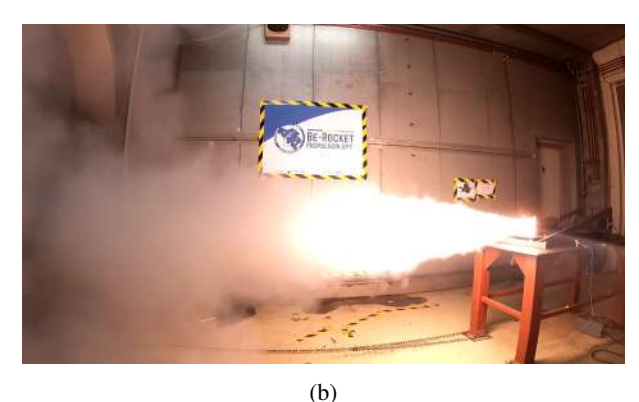


Figure 5: GoPro view of the static firing test: (a) PRO38 and (b) PRO75.

3.1 PRO38 results

The thrust data obtained from the PRO38 static tests is presented in Figure 6. The curves exhibit a high degree of consistency across tests, indicating reliable motor manufacturing and confirming the mechanical integrity and repeatability of the test bench. No significant structural deformation or signal anomalies were observed.

To assess the accuracy of the measurements, the cleanest thrust profile was compared to the manufacturer's reference curve, as shown in Figure 6. Both the shape and magnitude align closely, with minor deviations noted in the impulse values. Table 3 summarizes the results, showing slightly lower total and specific impulses than the reference, consistent with conservative performance margins. These outcomes validate both the acquisition system and the fidelity of the motor data.

Notable features include a sharper initial thrust peak in the experimental curve, attributed to the higher sampling rate of the acquisition system, likely capturing more instantaneous variations in thrust. Low-amplitude oscillations are visible in all tests, though Test 6 displays reduced oscillatory content, likely due to increased mechanical stiffness from unlubricated rails during that session. The presence of these oscillations may be due to combustion instabilities [9], though other minor hypotheses could also be considered, such as electrical noise induced in the signal by the wiring. Additionally, a small residual thrust is observed after the main burn, caused by the delay composition located at the forward end of the grain, which continues to combust briefly before triggering the ejection charge.

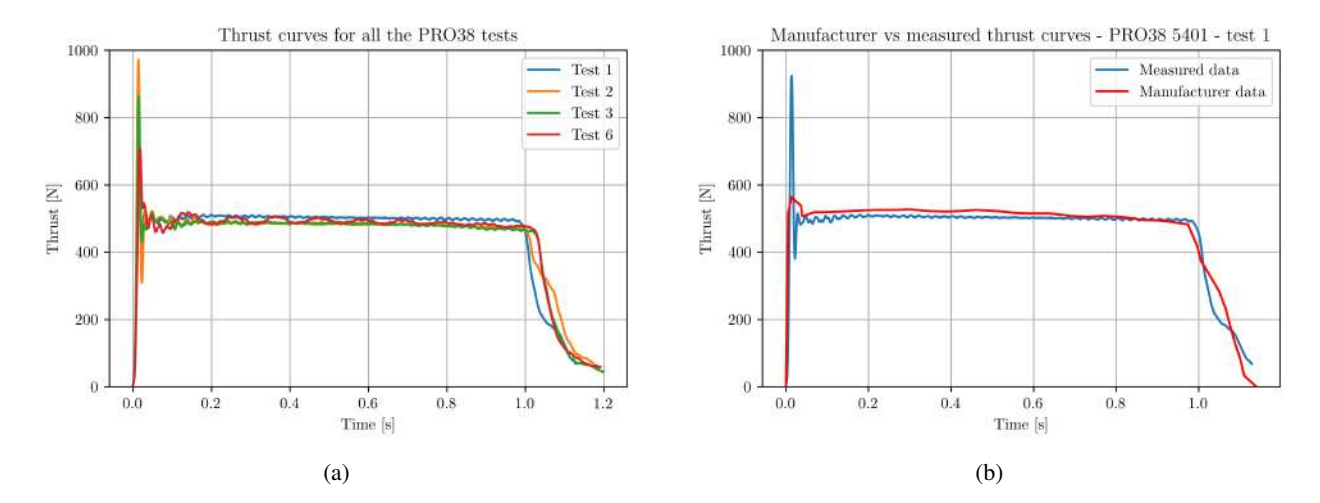


Figure 6: Thrust curves from the static firing tests of the PRO38 motor: (a) overlay of all test runs, and (b) comparison between manufacturer data and measured thrust curve from Test 1.

3.2 PRO75 results

The same analysis methodology was applied to the PRO75 motor tests. As shown in Figure 7, Tests 1 and 2 demonstrate consistent thrust profiles, while Test 3 deviates with a higher overall thrust and a secondary peak during the latter half of the burn. Although the cause remains inconclusive, a defect in the fuel grain was identified prior to the test, which likely contributed to the observed deviation. Additionally, GoPro footage from Test 3 captured a vertical shift of the test bench table coinciding with the onset of combustion instability around 1.25 s, though the causality between the two remains uncertain.

Test 2 in represented along with the manufacturer's reference curve in Figure 7, for a comparison basis. While the average thrust levels are in good agreement, the experimental thrust decays earlier than the reference, resulting in a reduced total impulse. As summarized in Table 3, this underperformance may be linked to aging effects in the propellant, as the motors were approaching the expiration date given by the manufacturer, potentially leading to reduced performance due to the composite propellant degradation.

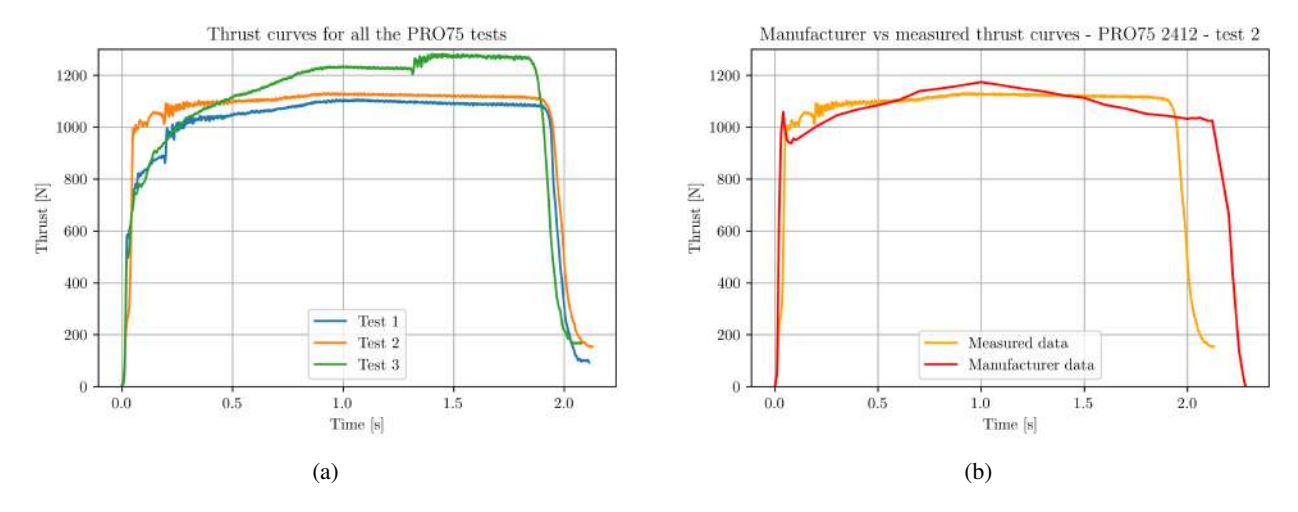


Figure 7: Thrust curves from the static firing tests of the PRO75 motor: (a) overlay of all test runs, and (b) comparison between manufacturer data and measured thrust curve from Test 1.

Model	Number	F_{max} [N]	F _{avg} [N]	t_b [s]	I _{tot} [Ns]	I_{sp} [s]
PRO38	Test 1	923.68	465.89	1.13	526.12	200.06
	Test 2	972.58	442.64	1.18	523.48	199.55
	Test 3	863.72	432.68	1.20	518.91	198.01
	Test 4	-	-	-	-	-
	Test 5	-	-	-	-	-
	Test 6	707.99	441.41	1.19	525.85	200.29
	Tests avg.	867.00	445.66	1.18	523.59	199.48
	Reference	555.21	472.18	1.14	540.10	222.80
	Error [%]	+56.15	-5.62	+3.51	-3.06	-10.47
PRO75	Test 1	1107.76	980.53	2.11	2071.50	176.12
	Test 2	1131.81	1025.54	2.13	2182.30	185.54
	Test 3	1283.68	1083.90	2.07	2247.93	191.12
	Tests avg.	1174.42	1029.99	2.10	2167.25	184.26
	Reference	1204	1113	2.12	2412	205
	Error [%]	2.47	-7.46	0.94	-10.15	-10.12

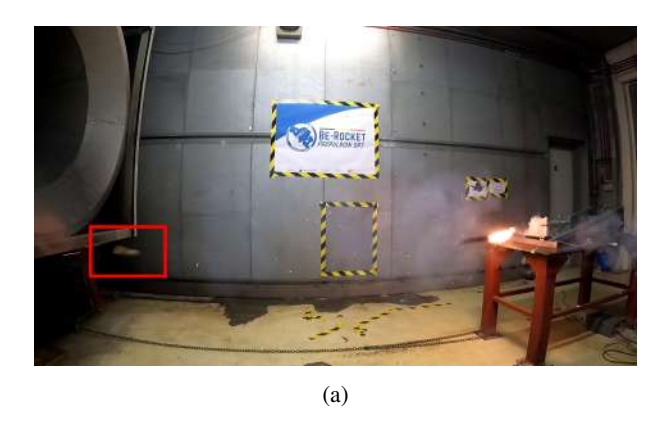
Table 3: Static fire tests results data.

3.3 Failed tests

During Test 4, an unintended ignition occurred due to an error in the LabVIEW control sequence, which left the ignition line active. As a result, the motor ignited without manual initiation of the test sequence. No thrust data were recorded, but safety protocols ensured that no personnel were present in the test room at the time. The issue was subsequently corrected in the control software to prevent recurrence.

In Test 5, the motor experienced another failure: the nozzle and propellant grains were ejected upon ignition. Figure 8 shows the grain burning outside the casing. The failure is attributed to insufficient tightening of the nozzle within the frame.

Both incidents highlighted critical areas for improvement in both control system design and assembly procedures. They reinforced the necessity of rigorous pre-test validation, comprehensive checklists, and continuous iteration on both hardware and software for future experimental campaigns.



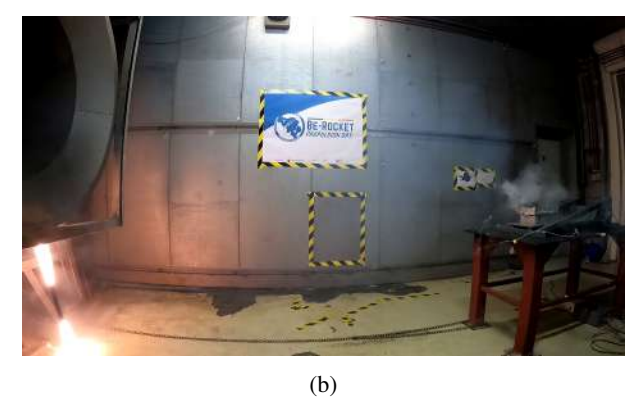


Figure 8: GoPro footage of the failed static Test 5 for the PRO38 motor. The failure was caused by the nozzle being ejected at ignition. (a) Frame showing the nozzle ejection immediately after the pressure rise, and (b) the propellant grain burning outside the motor casing.

4. Rocket launch

In October 2024, the Be-Rocket team successfully conducted the first launch of Bossart-I from the Elsenborn military base in Belgium. This inaugural mission was overall a great success for the team; however, a few issues occurred during the flight.

Firstly, the recovery parachute failed to deploy as intended, causing the rocket to impact the ground at an excessively high velocity. Secondly, due to the unavailability of the originally planned motor, the team was forced to select an alternative model shortly before the launch. The chosen substitute was the PRO75 2856 - 2G, which has the same dimensions but a slightly higher total impulse.

The simplified apogee prediction model estimated a maximum altitude of approximately 1439 m, while Bossart-I reached an actual apogee of 1474 m. This close agreement confirms the reliability of the model within the subsonic regime. It is important to note, however, that the prediction model does not account for transonic aerodynamic effects, which could become significant if the rocket exceeds the speed of sound.

Figure 9 shows a picture of the launch (left) and a 3D rendering of the rocket (right).





Figure 9: (a) First launch of *Bossart-I* at the Elsenborn military base in October 2024. (b) 3D rendering of the *Bossart-I* rocket.

5. Conclusions and future work

This work presents the experimental validation of solid rocket motors for the student-built Bossart-I sounding rocket. A simplified apogee prediction model was created to support the selection of appropriate SRMs for two flight objectives (1 km and 3 km), and its results were successfully benchmarked against OpenRocket simulations. Based on this analysis, the PRO75 2412 and PRO75 5880 motors were selected for testing and integration into the launch vehicle.

A dedicated and modular test bench was designed and installed at the Beauvechain Air Base, enabling the safe and repeatable static testing of multiple SRM configurations. The experimental campaign demonstrated good agreement with manufacturer thrust data and highlighted key lessons in ignition safety, system robustness, and test preparation. Despite a few test anomalies, the thrust measurement system and bench design were validated, showing sufficient fidelity.

The *Bossart-I* rocket was successfully launched in October 2024 from the Elsenborn military base, marking a key milestone for the Be-Rocket student team. This launch validated the design choices and experimental processes developed over the course of the project.

Future work will include upgrading to the 3 km motor, following the same test campaign steps for validation. In parallel, the team has initiated the development of a new rocket, *Bossart-II*, which is intended to integrate a Hybrid Rocket Engine (HRE).

Acknowledgments

We acknowledge the technicians of the ATM department of Université libre de Bruxelles, in particular Lionel Lambert and Florent Biname for their help, advice, and support for manufacturing and testing. We thank the 1st Wing of the Air Component of the Belgian Armed Forces for hosting our test bench in the Beauvechain Air Base. And finally, we thank all the members involved in Be-Rocket.

References

- [1] Be-Rocket Team. Be-rocket project website. https://www.berocket.be/. Accessed: 2025-06-13.
- [2] Cedric Dupont, Matthew Bullock, Michel Prevost, Raymond Bec, Yves Maisonneuve, Nicolas Pillet, and Roger Barenes. *The PERSEUS Student Launcher Project and Associated Hybrid Propulsion Activities*. 2012.
- [3] EuRoC Team. European rocketry challenge (euroc). https://euroc.pt/. Accessed: 2025-06-13.
- [4] Mattias Forsberg. New altitude record for student-built hybrid rocket, April 2023.
- [5] Stephen D. Heister, William E. Anderson, Timothée L. Pourpoint, and R. Joseph Cassady. *Rocket Propulsion*. Cambridge Aerospace Series. Cambridge University Press, 2019.
- [6] Sang-Hyeon Lee and Ralph C. Aldredge. Analytic approach to determine optimal conditions for maximizing altitude of sounding rocket: Flight in standard atmosphere. *Aerospace Science and Technology*, 46:374–385, 2015.
- [7] Ahmed Mahjub, Nurul Musfirah Mazlan, M. Z. Abdullah, and Qummare Azam. Design optimization of solid rocket propulsion: A survey of recent advancements. *Journal of Spacecraft and Rockets*, 57(1):3–11, 2020.
- [8] Taylor Moberly, Wesley Gillman, Adam Joseph, and Ilteris Demirkiran. An approach to student experience and knowledge development in rocket propulsion and support systems. In *SoutheastCon* 2016, pages 1–5, 2016.
- [9] Thomas B. O'Hara and Frank E. Marble. Chuffing and nonacoustic instability phenomena in solid propellant rockets. *Combustion Science and Technology*, 7(5-6):155–169, 1973.
- [10] TL Varghese. *The chemistry and technology of solid rocket propellants (a treatise on solid propellants)*, volume 1. Allied Publishers, 2017.